Naval Research Laboratory

Washington, DC 20375-5320

NRL/MR/6390--11-9320

Ground State Resonance Structure of Some Typical High Explosives Calculated by Density Functional Theory

L. HUANG

Center for Computational Materials Science
Materials Science and Technology Division

A. SHABAEV

George Mason University
Fairfax, Virginia

S.G. LAMBRAKOS
N. BERNSTEIN
V. JACOBS

Center for Computational Materials Science
Materials Science and Technology Division

D. FINKENSTADT

U.S. Naval Academy
Annapolis, Maryland

L. MASSA

Hunter College
New York, New York

March 4, 2011

REPORT DOCUMENTATION PAGE

Form Approved
OMB No. 0704-0188

1. REPORT DATE *(DD-MM-YYYY)*	**2. REPORT TYPE**	**3. DATES COVERED** *(From - To)*
04-03-2011	NRL Memorandum Report	01-03-2010 to 01-01-2011

4. TITLE AND SUBTITLE

Ground State Resonance Structure of Some Typical High Explosives Calculated by Density Functional Theory

5a. CONTRACT NUMBER

5b. GRANT NUMBER

5c. PROGRAM ELEMENT NUMBER

6. AUTHOR(S)

L. Huang, A. Shabaev,* S.G. Lambrakos, N. Bernstein, V. Jacobs, D. Finkenstadt,† and L. Massa‡

5d. PROJECT NUMBER

5e. TASK NUMBER

5f. WORK UNIT NUMBER

0305

7. PERFORMING ORGANIZATION NAME(S) AND ADDRESS(ES)

Naval Research Laboratory, Code 6394
4555 Overlook Avenue, SW
Washington, DC 20375-5320

8. PERFORMING ORGANIZATION REPORT NUMBER

NRL/MR/6390--11-9320

9. SPONSORING / MONITORING AGENCY NAME(S) AND ADDRESS(ES)

Office of Naval Research
One Liberty Center
875 North Randolph Street, Suite 1425
Arlington, VA 22203-1995

10. SPONSOR / MONITOR'S ACRONYM(S)

ONR

11. SPONSOR / MONITOR'S REPORT NUMBER(S)

12. DISTRIBUTION / AVAILABILITY STATEMENT

Approved for public release; distribution is unlimited.

13. SUPPLEMENTARY NOTES

*George Mason University, Department of Computation and Data Sciences, Fairfax, VA 22030
†U.S. Naval Academy, Physics Department, Annapolis, MD 21402
‡Hunter College, City University of New York, New York, NY 10065

14. ABSTRACT

We present calculations of ground state resonance structure associated with the high explosives β-HMX, PETN, RDX, TNT1 and TNT2 using density functional theory (DFT), which is for the construction of parameterized dielectric response functions for excitation by electromagnetic waves at compatible frequencies. These dielectric functions provide for different types of analyses concerning the dielectric response of explosives. In particular, these dielectric response functions provide quantitative initial estimates of spectral response features for subsequent adjustment with respect to additional information such as laboratory measurements and other types of theory based calculations. With respect to qualitative analysis, these spectra provide for the molecular level interpretation of response structure. The DFT software GAUSSIAN was used for the calculations of ground state resonance structure presented here.

15. SUBJECT TERMS

Density functional theory (DFT) Explosives
Dielectric functions

16. SECURITY CLASSIFICATION OF:			**17. LIMITATION OF ABSTRACT**	**18. NUMBER OF PAGES**	**19a. NAME OF RESPONSIBLE PERSON**
					Samuel G. Lambrakos
a. REPORT	**b. ABSTRACT**	**c. THIS PAGE**	UL	25	**19b. TELEPHONE NUMBER** *(include area code)*
Unclassified	Unclassified	Unclassified			(202) 767-2601

Contents

Ground State Resonance Structure of Some Typical High Explosives Calculated by Density Functional Theory

Introduction

A significant aspect of using response spectra calculated by density functional theory, DFT, for the direct construction of permittivity functions is that it adopts the perspective of computational physics, according to which a numerical simulation represents another source of "experimental" data. This perspective is significant in that a general procedure may be developed for construction of permittivity functions using DFT calculations as a quantitative initial estimate of spectral response features for subsequent adjustment with respect to additional information such as experimental measurements and other types of theory based calculations. That is to say, for the purpose of simulating many electromagnetic response characteristics of materials, DFT is sufficiently mature for the purpose of generating data complementing, as well as superseding, experimental measurements.

In the case of THz excitation of materials, the procedure of using response spectra calculated using DFT for the direct construction of permittivity functions is well posed owing to the physical characteristic of THz excitation. In particular, it is important to note that the procedure for constructing a permittivity function using response spectra calculated using DFT is physically consistent with the characteristically linear response associated with THz excitation of molecules. Accordingly, one observes a correlation between the advantages of using THz excitation for detection of IEDs (and ambient materials) and those for its numerical simulation based on DFT. Specifically, THz excitation is associated with frequencies that are characteristically perturbative to molecular states, in contrast to frequencies that can induce appreciable electronic state transitions. Of course, the practical aspect of the perturbative character of THz excitation for detection is that detection methodologies can be developed which do not damage materials under examination. The perturbative character of THz excitation with respect to molecular states has significant implications with respect to its numerical simulation based on DFT. It follows then that, owing to the perturbative character of THz excitation, which is characteristically linear, one is able to make a direct association between local oscillations about ground-state minima of a given molecule and THz excitation spectra.

In what follows, calculations are presented of ground state resonance structure associated with the high explosives β–HMX, PETN, RDX, TNT1 and TNT2 using DFT. This resonant structure is for the construction of parameterized dielectric response functions for excitation by electromagnetic waves at compatible frequencies. For this purpose the DFT software GAUSSIAN09 (G09) was adopted [1].

The organization of the subject areas presented here are as follows. First, a general review of the elements of vibrational analysis using DFT that are relevant for the calculation of absorption spectra is presented. Second, a general review is presented concerning the formal structure of permittivity functions in terms of analytic function representations. An understanding of the formal structure of permittivity functions in terms of both physical consistency and causality is important for post-processing of DFT calculations for the purpose of constructing permittivity functions. Third, information concerning the ground state resonance structure of the explosives β–HMX, PETN, RDX, TNT1 and TNT2, which is obtained using DFT, is presented as a set of case studies. This information consists of the ground state molecular geometry and response spectrum for an isolated molecule. In addition, for each of the explosives, a prototype calculation is presented to demonstrate the construction of parameterized permittivity functions using response spectra calculated using DFT.

Manuscript approved January 14, 2011.

Construction of Permittivity Functions using DFT

Density Functional Theory

The application of density functional theory (DFT) and related methodologies for the determination of electromagnetic response characteristics is important for the analysis of parameter sensitivity. That is to say, many characteristics of the electromagnetic response of a given material may not be detectable, or in general, not relevant for detection. Accordingly, sensitivity analyses concerning the electromagnetic response of layered composite systems can adopt the results of simulations using DFT, and related methodologies, to provide realistic limits on detectability that are independent of a specific system design for IED detection. In addition, analysis of parameter sensitivity based on atomistic response characteristics of a given material, obtained by DFT, provide for an "optimal" best fit of experimental measurements for the construction of permittivity functions. It follows that within the context of parameter sensitivity analysis, data obtained by means of DFT represents a true complement to data that has been obtained by means of experimental measurements.

The DFT software GAUSSIAN09 (G09) can be used to compute an approximation of the IR absorption spectrum of a molecule [1]. This program calculates vibrational frequencies by determining second derivatives of the energy with respect to the Cartesian nuclear coordinates, and then transforming to mass-weighted coordinates at a stationary point of the geometry. [2]. The IR absorption spectrum is obtained using density functional theory to compute the ground state electronic structure in the Born-Oppenheimer approximation using Kohn-Sham density functional theory [3-7]. GAUSSIAN uses specified orbital basis functions to describe the electronic wavefunctions and density. For a given set of nuclear positions, the calculation directly gives the electronic charge density of the molecule, the potential energy *V*, and the displacements in Cartesian coordinates of each atom. The procedure for vibrational analysis followed in GAUSSIAN is that described in [8]. Reference [9] presents a fairly detailed review of this procedure. A brief description of this procedure is as follows.

The procedure followed by GAUSSIAN is based on the fact the vibrational spectrum depends on the Hessian matrix $\mathbf{f}_{\mathrm{CART},}$ which is constructed using the second partial derivatives of the potential energy *V* with respect to displacements of the atoms in Cartesian coordinates. Accordingly, the elements of the *3N* x *3N* matrix $\mathbf{f}_{\mathrm{CART}}$ are given by

$$f_{\mathrm{CART}ij} = \left(\frac{\partial^2 V}{\partial \xi_i \partial \xi_j} \right)_0 \tag{1}$$

where $\{\xi_1,\xi_2,\xi_3,\xi_4,\xi_5,\xi_6,...,\xi_{3N}\} = \{\Delta x_1,\Delta y_1,\Delta z_1,\Delta x_2,\Delta y_2,\Delta z_2,...,\Delta z_N\}$, which are displacements in Cartesian coordinates, and *N* is the number of atoms. As discussed above, the zero subscript in Eq.(1) indicates that the derivatives are taken at the equilibrium positions of the atoms, and that the first derivatives are zero. Given the Hessian matrix defined by Eq.(1) the operations for calculation of the vibrational spectrum require that the Hessian matrix Eq.(1) be transformed to mass-weighted Cartesian coordinates according to the relation

$$f_{\mathrm{MWC}ij} = \frac{f_{\mathrm{CART}ij}}{\sqrt{m_i m_j}} = \left(\frac{\partial^2 V}{\partial q_i \partial q_j} \right)_0 \tag{2}$$

where $\{q_1,q_2,q_3,q_4,q_5,q_6,...,q_{3N}\} = \left\{\sqrt{m_1}\Delta x_1,\sqrt{m_1}\Delta y_1,\sqrt{m_1}\Delta z_1,\sqrt{m}_2\Delta x_2,\sqrt{m_2}\Delta y_2,\sqrt{m_2}\Delta z_2,...,\sqrt{m_N}\Delta z_N\right\}$ are the mass-weighted Cartesian coordianates. GAUSSIAN computes the energy second derivatives Eq.(2), thus computing the forces for displacement perturbations of each atom along each Cartesian direction. The first derivatives of the dipole moment with respect to atomic positions $\partial\bar{\mu}/\partial\xi_i$ are also computed. Each vibrational eigenmode leads to one peak in the absorption spectrum, at a frequency equal to the

mode's eigenfrequency ν_i. The absorption intensity corresponding to a particular eigenmode *i* whose eigenfrequency is ν_i is given by

$$I_i = \frac{\pi}{3c}\left|\sum_{k=1}^{3N}\frac{\partial\vec{\mu}}{\partial\xi_k}l_{\mathrm{CART}ki}\right|^2, \tag{3}$$

where $\mathbf{l}_{\mathrm{CART}}$ is the matrix whose elements are the displacements of the atoms in Cartesian coordinates and the normalization constant N_i is given by

$$N_i = \sqrt{\sum_{k=1}^{3N} l_{\mathrm{CART}ki}^2} \quad . \tag{4}$$

The matrix $\mathbf{l}_{\mathrm{CART}}$ is determined by the following procedure. First,

$$\mathbf{l}_{\mathrm{CART}} = \mathbf{M}\mathbf{l}_{\mathrm{MWC}}\,, \tag{5}$$

where $\mathbf{l}_{\mathrm{MWC}}$ is the matrix whose elements are the displacements of the atoms in mass-weighted Cartesian coordinates and **M** is a diagonal matrix defined by the elements

$$M_{ii} = \frac{1}{\sqrt{m_i}}\,. \tag{6}$$

Proceeding, $\mathbf{l}_{\mathrm{MWC}}$ is the matrix needed to diagonalize $\mathbf{f}_{\mathrm{MWC}}$ defined by Eq.(2) such that

$$(\mathbf{l}_{\mathrm{MWC}})^{\mathrm{T}}\,\mathbf{f}_{\mathrm{MWC}}(\mathbf{l}_{\mathrm{MWC}}) = \Lambda\,, \tag{7}$$

where Λ is the diagonal matrix with eigenvalues λ_i. The procedure for diagonalizing Eq.(7) consists of the operations

$$\mathbf{f}_{\mathrm{INT}} = (\mathbf{D})^{\mathrm{T}}\,\mathbf{f}_{\mathrm{MWC}}(\mathbf{D}) \tag{8}$$

and

$$(\mathbf{L})^{\mathrm{T}}\,\mathbf{f}_{\mathrm{MWC}}(\mathbf{L}) = \Lambda\,, \tag{9}$$

where **D** is a matrix transformation to coordinates where rotation and translation have been separated out and **L** is the transformation matrix composed of eigenvectors calculated according to Eq.(9). The eigenfrequencies in units of (cm^{-1}) are calculated using the eigenvalues λ_i by the expression

$$\nu_i = \sqrt{\frac{\lambda_i}{4\pi^2c^2}}\,, \tag{10}$$

where *c* is the speed of light. The elements of $\mathbf{l}_{\mathrm{CART}}$ are given by

$$l_{\mathrm{CART}ki} = \sum_{j=1}^{3N}\frac{D_{kj}L_{ji}}{\sqrt{m_j}}\,, \tag{11}$$

where *k, i=1,…, 3N,* and the column vectors of these elements are the normal modes in Cartesian coordinates.

The intensity Eq.(3) must then be multiplied by the number density of molecules to give an absorption strength. It follows that the absorption spectrum calculated by GAUSSIAN is a sum of delta functions whose positions and magnitudes correspond to the vibrational frequencies and magnitudes, respectively. In principle, however, these spectral components must be broadened and shifted to account for anharmonic effects such as finite mode lifetimes and inter-mode couplings.

Dielectric Permittivity Functions

The general approach of constructing permittivity functions according to the best fit of available data for given material corresponding to many different types of experimental measurements is not unprecedented and has been typically the dominant approach, e.g., the permittivity function of water. The general simulation framework presented here considers an extension of this approach in that calculations of electromagnetic response based on DFT is also adopted as data for construction of permittivity functions. The inclusion of this type of information is significant for accessing what spectral response features at the molecular level are actually detectable with respect to a given set of detection parameters. Accordingly, permittivity functions having been constructed using DFT calculations provide a quantitative correlation between macroscopic material response and molecular structure. Within this context it is not important that the permittivity function be quantitatively accurate for the purpose of being adopted as input for system simulation. Rather, it is important that the permittivity function be qualitatively accurate in terms of specific dielectric response features for the purpose of sensitivity analysis, which is relevant for the assessment of absolute detectability of different types of molecular structure with respect to a given set of detection parameters. That is to say, permittivity functions that have been determined using DFT can provide a mechanistic interpretation of material response to electromagnetic excitation that could establish the well posedness of a given detection methodology for detection of specific molecular characteristics. Within the context of practical application, permittivity functions having been constructed according to the best fit of available data would be “correlated” with those obtained using DFT for proper interpretation of permittivity-function features. Subsequent to establishment of good correlation between DFT and experiment, DFT calculations can be adopted as constraints for the purpose of constructing permittivity functions, whose features are consistent with molecular level response, for adjustment relative to specific sets of either experimental data or additional molecular level information.

The construction of permittivity functions using DFT calculations involves, however, an aspect that requires serious consideration. This aspect concerns the fact that a specific parametric function representation must be adopted. Accordingly, any parametric representation, i.e., parameterization, adopted for permittivity-function construction must be physically consistent with specific molecular response characteristics, while limiting the inclusion of feature characteristics that tend to mask response signatures that may be potentially detectable.

In principle, parameterizations are of two classes. One class consists of parameterizations that are directly related to molecular response characteristics. This class of parameterizations would include spectral scaling and width coefficients. The other class consists of parameterizations that are purely phenomenological and are structured for optimal and convenient best fits to experimental measurements. A sufficiently general parameterization of permittivity functions is given by Drude-Lorentz approximation [10]

$$\varepsilon(\nu) = \varepsilon_r(\nu) + i\varepsilon_i(\nu) = \varepsilon_\infty + \sum_{n=1}^{N} \frac{\nu_{np}^2}{(\nu_{no}^2 - \nu^2) - i\gamma_n \nu} \ , \tag{12}$$

where ν_{np} and γ_n are the spectral scaling and width of a resonance contributing to the permittivity function. The permittivity ε_∞ is a constant since the dielectric response at high frequencies is

substantially detuned from the probe frequency. The real and imaginary parts, $\varepsilon_r(\nu)$ and $\varepsilon_i(\nu)$, respectively, of the permittivity function can be written separately as

$$\varepsilon_r(\nu) = \varepsilon_\infty + \sum_{n=1}^{N} \frac{\nu_{np}^2(\nu_{no}^2 - \nu^2)}{(\nu_{no}^2 - \nu^2)^2 + \gamma_n^2\nu^2} \quad \text{and} \quad \varepsilon_i(\nu) = \sum_{n=1}^{N} \frac{\nu_{np}^2\gamma_n\nu}{(\nu_{no}^2 - \nu^2)^2 + \gamma_n^2\nu^2} \ . \tag{13}$$

With respect to practical application, the absorption coefficient α and index of refraction n_r, given by

$$\alpha = \frac{4\pi\nu}{\sqrt{2}}\left[-\varepsilon_r + \sqrt{\varepsilon_r^2 + \varepsilon_i^2}\right]^{1/2} \quad \text{and} \quad n_r = \frac{1}{\sqrt{2}}\left[\varepsilon_r + \sqrt{\varepsilon_r^2 + \varepsilon_i^2}\right]^{1/2}, \tag{14}$$

respectively, provide direct relationships between calculated quantities obtained by DFT and the "conveniently measurable" quantities α and n_r.

Case Study 1: β – HMX

In this section are presented two sets of data, which are the results of computational experiments using DFT, concerning the molecule β – HMX. These are the relaxed or equilibrium configuration of a single isolated molecule of β – HMX (see Table 1) and ground-state oscillation frequencies and IR intensities for this configuration that are calculated by DFT according to the frozen phonon approximation (see Table 2). For these calculations geometry optimization and vibrational analysis was effected using the DFT model B3LYP [11, 12] and basis function 6-311++G(2d,2p) [13]. According to the specification of this basis function, the symbol "**++**" designates the 6-311G basis set supplemented by diffuse functions [14], and (2d,2p) designates polarization functions having 2 sets of d functions for heavy atoms and 2 sets of p functions for hydrogen atoms [15]. A schematic representation of the molecular geometry of β – HMX is shown in Fig.(1).

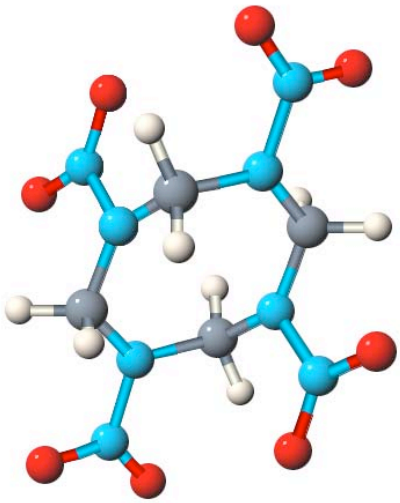

Figure 1. Molecular Geometry of β – HMX.

Shown in Fig.(2) is the IR intensity as a function of frequency for β – HMX according to a frozen phonon approximation. For the spectrum shown in Fig.(2), the structure of each resonance response is approximated essentially by that of a delta function.

Table 1. Atomic positions of β – HMX (Å)

Atomic number	X	Y	Z	Atomic number	X	Y	Z
6	-0.247569	2.398888	-0.24206	8	-0.481761	2.084279	-2.852395
6	-2.063866	0.625101	-0.034283	8	-2.079477	0.60568	-2.657757
6	1.429414	0.449077	-0.072891	8	1.610321	3.877071	0.675548
6	-0.386827	-1.324705	0.135093	8	3.18386	2.364102	0.605726
7	-1.131623	1.421861	-0.823793	8	-2.244633	-2.802996	-0.782467
7	1.122469	1.866827	-0.101235	8	-3.818203	-1.290037	-0.712928
7	0.497123	-0.347527	0.716733	1	-0.643824	2.678988	0.732229
7	-1.756822	-0.79264	-0.00604	1	-0.208649	3.282257	-0.86844
7	0.608684	-0.301254	2.107395	1	-3.075188	0.711052	-0.417038
7	-1.242997	1.375573	-2.214453	1	-2.026551	1.032712	0.973025
7	2.039759	2.752548	0.444065	1	0.009539	-1.605043	-0.839084
7	-2.674091	-1.678436	-0.551159	1	-0.425827	-2.207929	0.761672
8	-0.152503	-1.009914	2.74544	1	2.440755	0.363063	0.309801
8	1.445216	0.468641	2.550583	1	1.392	0.0414	-1.080169

Table 2. Oscillation frequencies and IR intensities:

Frequency cm^{-1}	Intensity (KM/Mol)	Frequency cm^{-1}	Intensity (KM/Mol)	Frequency cm^{-1}	Intensity (KM/Mol)	Frequency cm^{-1}	Intensity (KM/Mol)
20.5974	4.4642	423.5457	0.0001	958.1357	275.8733	1439.7352	12.4616
46.5227	6.2401	424.4072	6.6649	958.7657	0.0321	1455.7355	0
59.4169	0	595.4743	0	1078.5529	0.0015	1479.3719	0.0002
64.9626	2.6874	598.3283	38.8195	1084.0758	134.3721	1480.1064	48.3128
65.5097	0.0005	628.1299	32.6053	1154.6108	191.9206	1494.9257	0
91.0091	0	632.9158	0	1192.3604	0	1499.1006	95.5194
95.7746	0.4885	653.1038	5.7687	1219.5098	0	1597.9156	0.012
116.2327	0	655.3446	0	1233.8676	170.6558	1603.1827	654.1091
123.5112	0.5691	733.673	0	1261.0272	96.8792	1615.2202	0.024
155.7534	0	763.9167	13.9813	1261.6361	0.01	1617.4993	690.7993
165.5881	10.9519	769.637	0	1288.3562	0.0001	3080.0298	0.0009
202.3398	20.9064	776.5606	20.6047	1296.1097	977.5485	3081.1194	9.6204
220.1601	0	776.9724	0.0013	1310.3824	472.4158	3098.6262	25.9659
273.6165	0	783.8961	20.1101	1338.5525	0	3098.9294	0.0053
296.5221	0	839.4502	0.0003	1338.9509	0	3158.0271	0.0172
340.787	7.1838	840.1406	5.2862	1352.0732	20.0148	3158.1956	11.0469
344.5913	0	877.9347	15.0169	1374.7476	0.1501	3161.4685	4.0618
377.1029	6.4205	888.8403	0	1374.8451	17.9345	3161.7092	0.002
400.4941	0.0002	942.4828	289.7913	1404.5298	0		
402.1082	5.773	947.8026	0.0006	1426.7612	47.7131		

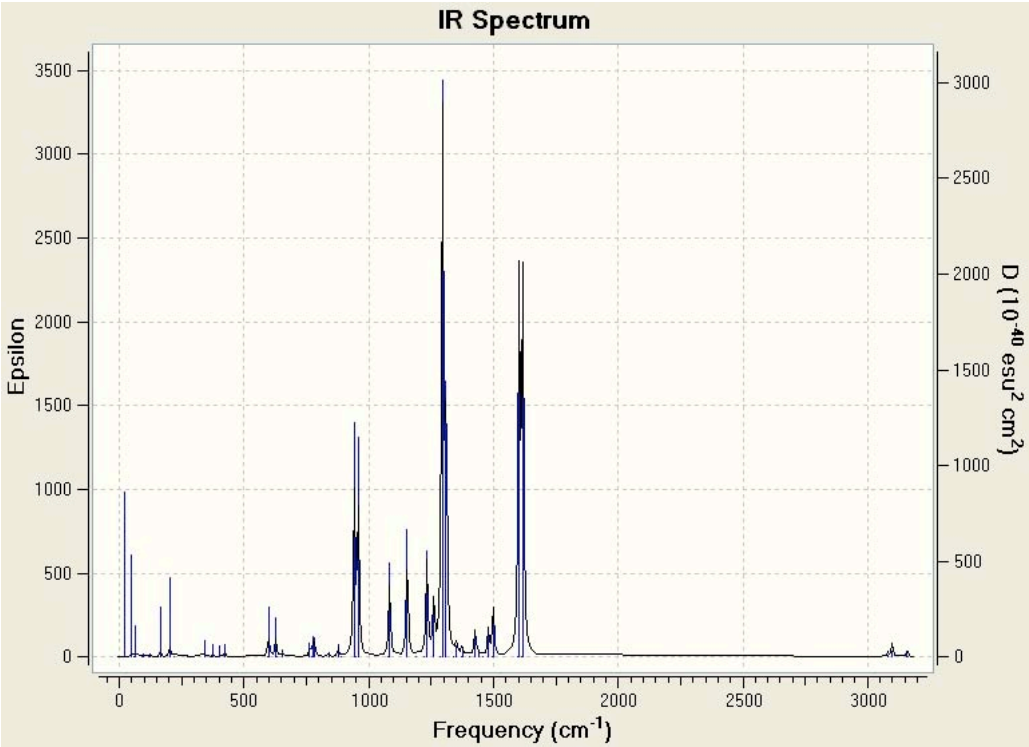

Figure 2. IR intensity as a function of frequency calculated using DFT B3LYP/6-311++G(2d,2p) for β-HMX according to frozen phonon approximation.

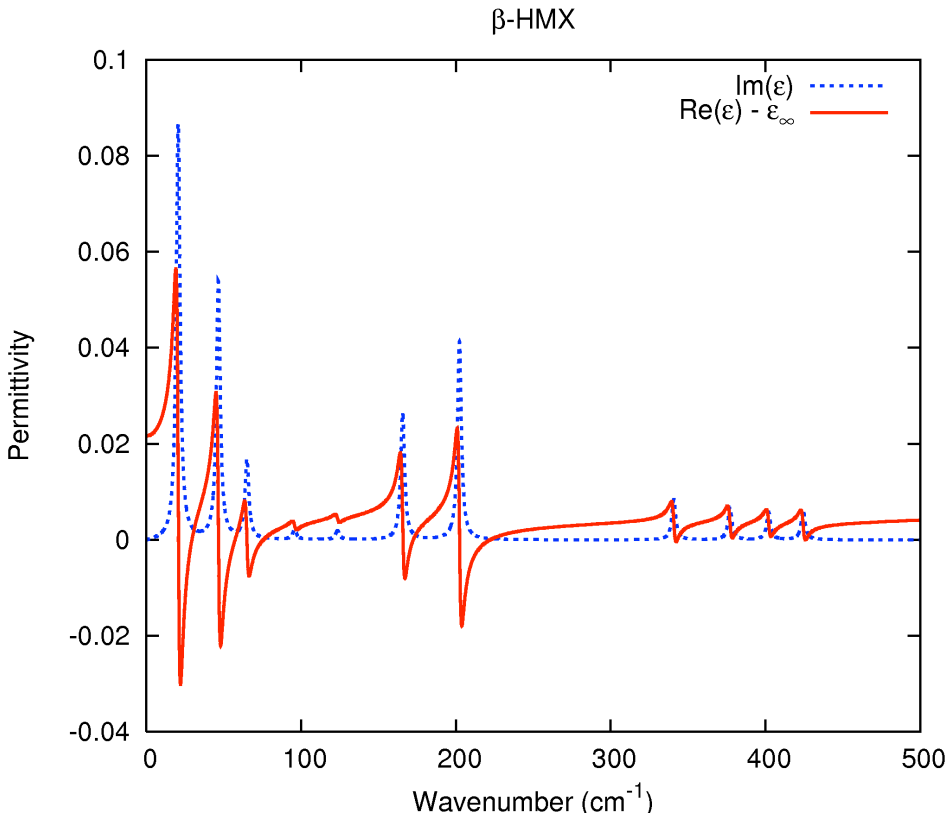

Figure 3. Real (solid) and imaginary (dashed) parts of permittivity function of β–HMX molecules with γ_n = 3 cm^{-1} and $\rho = 2.4 \cdot 10^{19}$ cm^{-3} for frequencies within THz range.

Case Study 2: PETN

In this section are presented two sets of data, which are the results of computational experiments using DFT, concerning the molecule PETN. These are the relaxed or equilibrium configuration of a single isolated molecule of PETN (see Table 3) and ground-state oscillation frequencies and IR intensities for this configuration that are calculated by DFT according to the frozen phonon approximation (see Table 4). The DFT model and basis function used for these calculations are the same as those used in case study 1. A schematic representation of the molecular geometry of PETN is shown in Fig.(4).

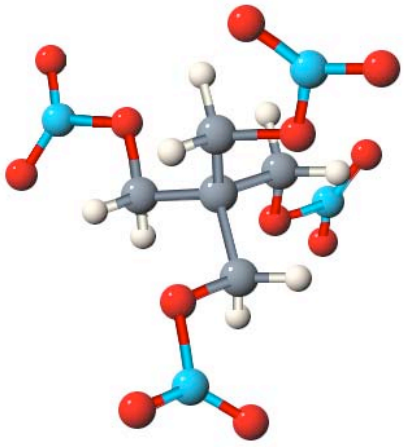

Figure 4. Molecular Geometry of PETN.

Shown in Fig.(5) is the IR intensity as a function of frequency calculated using DFT for PETN according to a frozen phonon approximation. For the spectrum shown in Fig.(5), the structure of each resonance response is approximated essentially by that of a delta function.

Table 3. Atomic positions of PETN (Å).

Atomic number	X	Y	Z	Atomic number	X	Y	Z
6	-0.89008	0.487044	0.169443	8	1.885603	-3.148164	-0.06536
6	0.56833	0.025631	0.355901	8	2.801652	-1.246607	0.487954
6	-0.954153	2.010353	0.393203	1	-1.969444	2.373078	0.253141
6	-1.775405	-0.266852	1.180709	1	-0.289344	2.531375	-0.29121
6	-1.399001	0.17896	-1.25209	1	0.903906	0.201954	1.374781
8	-0.536524	2.246621	1.753563	1	1.224466	0.550575	-0.333979
8	0.594489	-1.388358	0.071682	1	-1.43301	-0.084138	2.196278
8	-3.114945	0.243543	1.019535	1	-1.763653	-1.336176	0.985073
8	-0.503707	0.845656	-2.165744	1	-2.410743	0.55161	-1.391197
8	-5.169236	0.102355	1.756224	1	-1.382201	-0.89204	-1.438315
8	-3.660475	-1.176108	2.678384	7	-4.069163	-0.341502	1.911776
8	-0.213539	3.790051	3.268901	7	-0.561634	3.625752	2.13612
8	-0.916392	4.418249	1.301021	7	1.895046	-1.976796	0.177844
8	-0.065066	1.202636	-4.278301	7	-0.825239	0.640236	-3.54537
8	-1.784867	-0.046988	-3.786458				

Table 4. Oscillation frequencies and IR intensities:

Frequency cm^{-1}	Intensity (KM/Mol)	Frequency cm^{-1}	Intensity (KM/Mol)	Frequency cm^{-1}	Intensity (KM/Mol)	Frequency cm^{-1}	Intensity (KM/Mol)
24.1944	2.0809	316.0741	0	923.26	9.1634	1410.9082	32.0286
25.1486	0.0001	449.6382	3.5611	945.7603	8.2868	1422.7894	0.0001
39.6217	0.1006	449.678	3.56	945.7964	8.3144	1514.4496	0
40.7946	1.0765	531.1423	17.475	1009.2443	0.0001	1515.8597	6.4408
40.8093	1.078	586.0232	0	1018.9313	69.2683	1519.5519	17.4451
48.8877	0	616.7118	12.0616	1018.9486	69.3583	1519.5752	17.4574
50.6657	0.0052	621.5385	11.9061	1057.7988	110.9231	1704.4698	0.0468
55.4863	1.7452	621.5649	11.9235	1061.3842	0	1706.0529	293.7907
55.508	1.7454	671.4305	0	1182.1622	2.0461	1707.5656	669.1497
124.2462	0.5941	707.5737	66.0545	1201.7557	0.075	1707.6	669.3272
124.2875	0.594	707.6072	66.0823	1201.7788	0.0741	3085.7715	7.5588
132.7604	1.1955	754.7934	71.5529	1270.1554	0.0002	3086.3389	5.5306
145.448	0	769.8139	11.3843	1288.5605	44.1673	3086.384	5.5486
172.1583	0	769.8161	11.352	1288.6211	44.2379	3088.3333	0.0006
190.9592	1.002	770.3806	0.0003	1303.6309	425.1637	3139.4114	0.0009
191.0142	1.0007	771.5349	33.3462	1311.3896	290.9257	3141.219	4.1267
208.874	0	839.1219	0	1311.4103	291.0257	3141.3005	4.1112
248.6994	1.8583	847.8259	385.5923	1325.2662	0.0001	3143.2476	6.39
250.9887	1.5616	847.8293	385.3134	1334.1466	80.9233		
251.031	1.5589	851.4825	768.282	1406.0359	21.6309		
306.1457	1.222	879.0186	0.0002	1406.0658	21.5905		

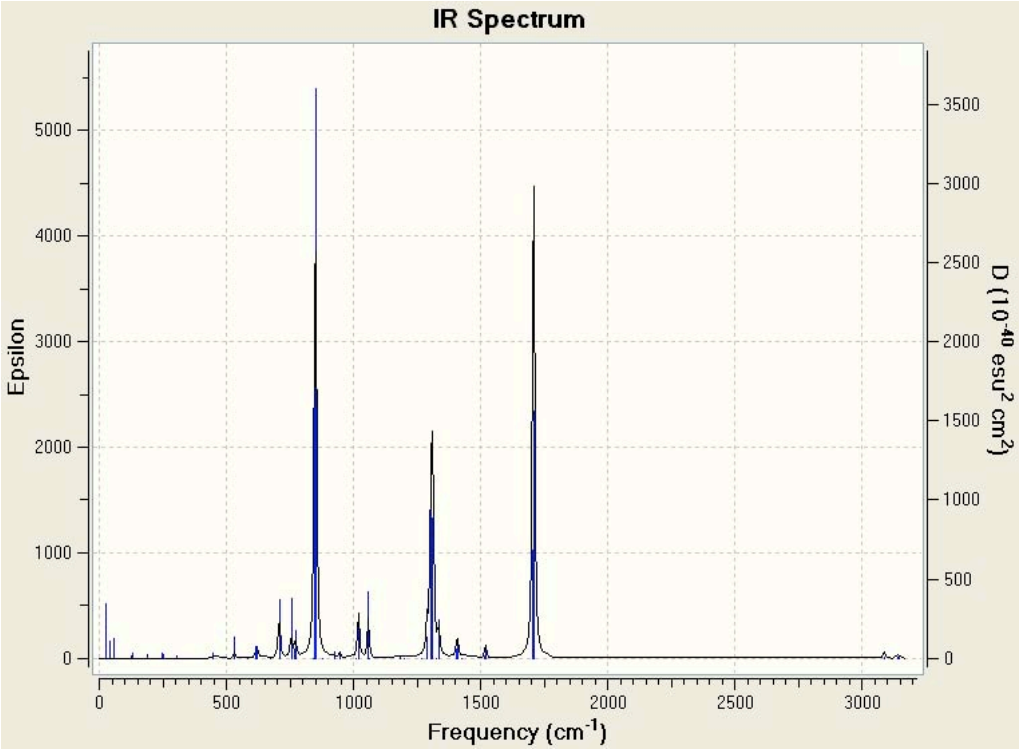

Figure 5. IR intensity as a function of frequency calculated using DFT B3LYP/6-311++G(2d,2p) for PETN according to frozen phonon approximation.

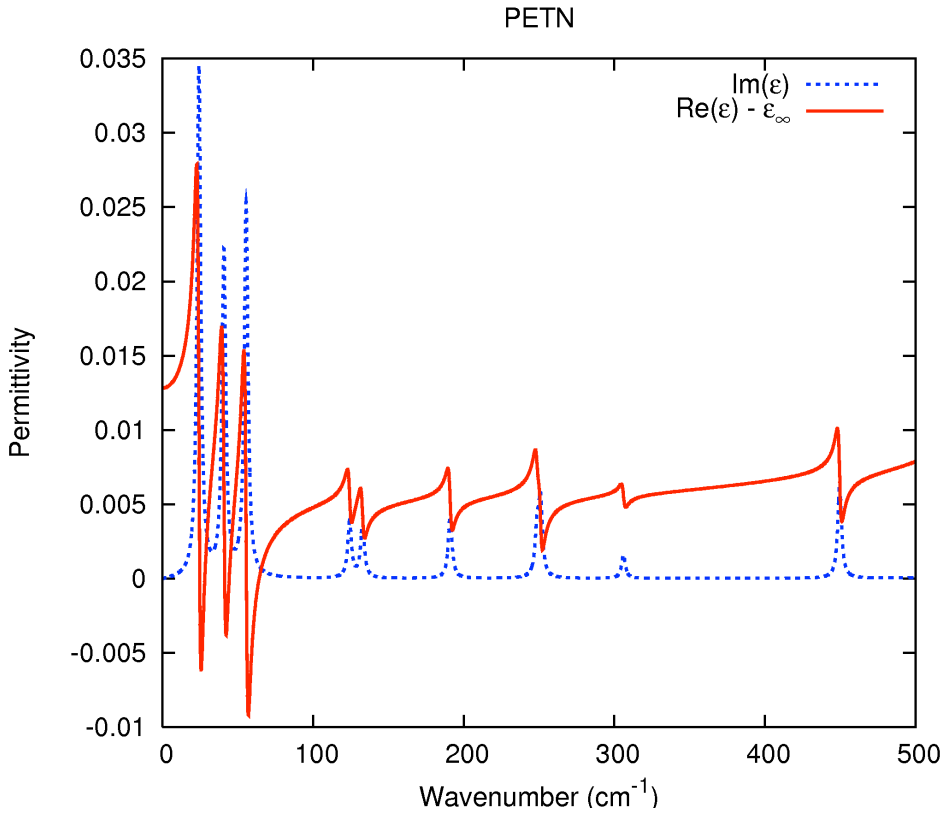

Figure 6. Real (solid) and imaginary (dashed) parts of permittivity function of PETN molecules with $\gamma_n = 3$ cm^{-1} and $\rho = 2.4 \cdot 10^{19}$ cm^{-3} for frequencies within THz range.

Case Study 3: RDX

In this section are presented two sets of data, which are the results of computational experiments using DFT, concerning the molecule RDX. These are the relaxed or equilibrium configuration of a single isolated molecule of RDX (see Table 5) and ground-state oscillation frequencies and IR intensities for this configuration that are calculated by DFT according to the frozen phonon approximation (see Table 6).). The DFT model and basis function used for these calculations are the same as those used in case study 1. A schematic representation of the molecular geometry of RDX is shown in Fig.(7).

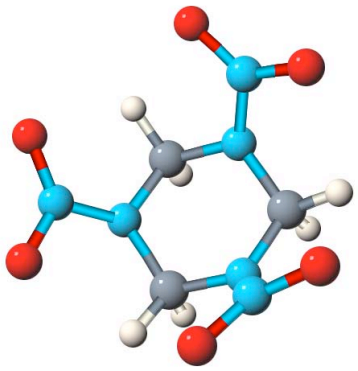

Figure 7. Molecular Geometry of RDX.

Shown in Fig.(8) is the IR intensity as a function of frequency calculated using DFT for RDX according to a frozen phonon approximation. For the spectrum shown in Fig.(8), the structure of each resonance response is approximated essentially by that of a delta function.

Table 5. Atomic positions of RDX (Å):

Atomic number	X	Y	Z	Atomic number	X	Y	Z
7	1.177132	-0.800831	0.102459	8	-1.148702	1.861918	2.523892
7	0.102459	1.177132	-0.800831	8	3.333613	-0.184585	0.086238
7	-0.800831	0.102459	1.177132	8	0.086238	3.333613	-0.184585
7	2.436639	-0.679768	0.742611	8	-0.184585	0.086238	3.333613
7	0.742611	2.436639	-0.679768	1	-1.515435	1.871323	0.32473
7	-0.679768	0.742611	2.436639	1	0.32473	-1.515435	1.871323
6	-1.083455	0.93108	0.011066	1	1.871323	0.32473	-1.515435
6	0.011066	-1.083455	0.93108	1	-1.794386	0.385919	-0.609699
6	0.93108	0.011066	-1.083455	1	-0.609699	-1.794386	0.385919
8	2.523892	-1.148702	1.861918	1	0.385919	-0.609699	-1.794386
8	1.861918	2.523892	-1.148702				

Table 6. Oscillation frequencies and IR intensities:

Frequency cm^{-1}	Intensity (KM/Mol)	Frequency cm^{-1}	Intensity (KM/Mol)	Frequency cm^{-1}	Intensity (KM/Mol)	Frequency cm^{-1}	Intensity (KM/Mol)
36.3016	0.0457	589.5756	12.0529	1008.1423	52.0064	1466.3945	29.2759
36.3016	0.0455	589.5756	12.0501	1008.1423	52.0228	1466.3945	29.2705
65.6946	0.2773	593.3556	0.0005	1137.1893	0.0007	1484.9159	77.5386
66.7914	0.7854	660.3034	3.91	1246.0972	19.5343	1605.9512	0.0006
100.3213	0.0217	660.3034	3.9149	1247.9865	60.5211	1637.2725	455.8935
100.3213	0.0216	755.2321	0.2018	1247.9865	60.5168	1637.2725	455.9394
219.7949	5.4286	764.2693	0.1606	1278.0071	0	3070.623	0.8397
219.7949	5.4314	764.2693	0.161	1289.4368	183.7337	3070.623	0.8394
303.525	0.0004	785.2931	90.7195	1289.4368	183.787	3076.4897	37.061
362.7641	0.2746	859.1682	0.2644	1342.053	338.9161	3201.8977	14.7538
362.7641	0.2747	859.1682	0.2644	1368.4448	0.0158	3201.8977	14.7445
407.6598	0.7931	887.6022	25.785	1385.4041	3.3489	3204.033	16.1921
407.6598	0.7951	909.5884	292.0052	1385.4041	3.3494		
437.1534	11.3308	909.5884	291.9845	1407.8136	17.1052		
457.0457	21.8362	938.4995	118.3704	1407.8136	17.1032		

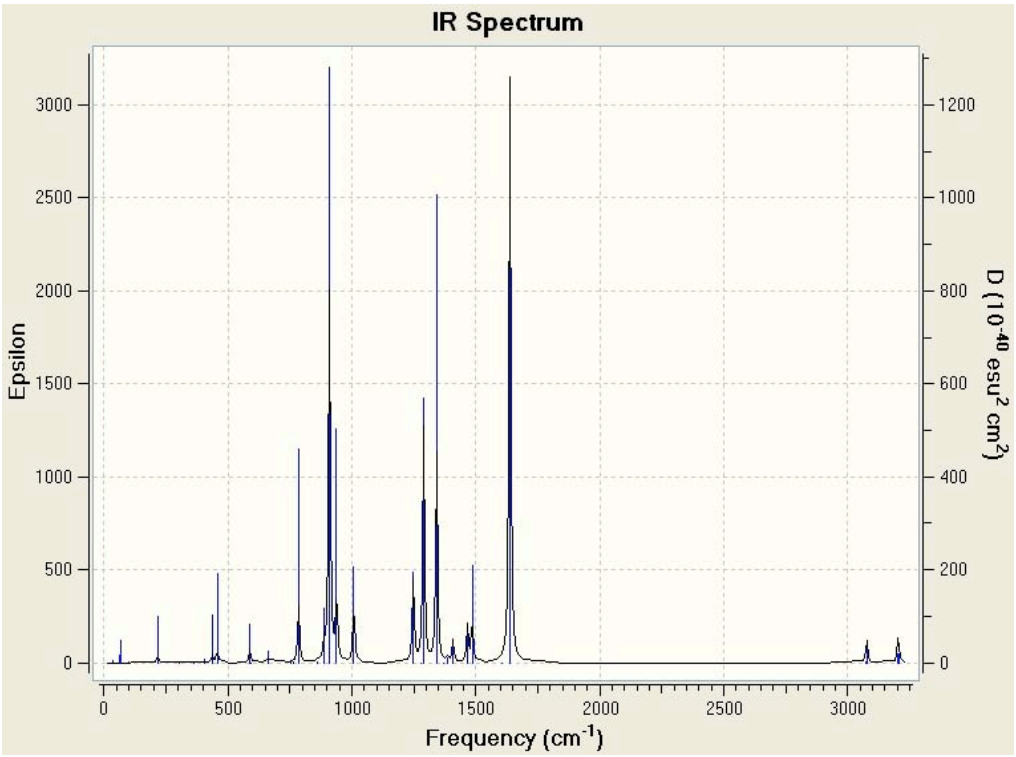

Figure 8. IR intensity as a function of frequency calculated using DFT B3LYP/6-311++G(2d,2p) for RDX according to frozen phonon approximation.

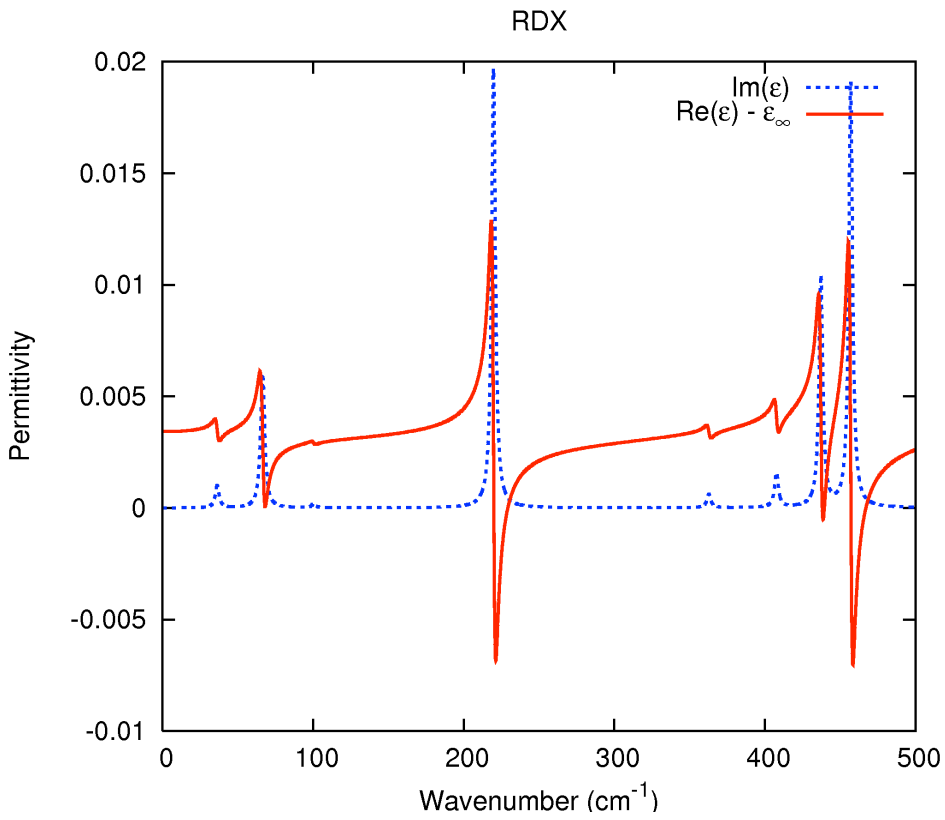

Figure 9. Real (solid) and imaginary (dashed) parts of permittivity function of RDX molecules with γ_n = 3 cm^{-1} and $\rho = 2.4 \cdot 10^{19}$ cm^{-3} for frequencies within THz range.

Case Study 4: TNT1

In this section are presented two sets of data, which are the results of computational experiments using DFT, concerning the molecule TNT1. These are the relaxed or equilibrium configuration of a single isolated molecule of TNT1 (see Table 7) and ground-state oscillation frequencies and IR intensities for this configuration that are calculated by DFT according to the frozen phonon approximation (see Table 8). The DFT model and basis function used for these calculations are the same as those used in case study 1. A schematic representation of the molecular geometry of TNT1 is shown in Fig.(10).

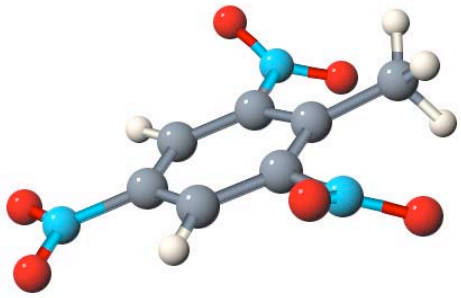

Figure 10. Molecular Geometry of TNT1.

Shown in Fig.(11) is the IR intensity as a function of frequency calculated using DFT for TNT1 according to a frozen phonon approximation. For the spectrum shown in Fig.(11), the structure of each resonance response is approximated essentially by that of a delta function.

Table 7. Atomic positions of TNT1 (Å):

Atomic number	X	Y	Z	Atomic number	X	Y	Z
1	1.294359	-0.627693	1.916458	6	1.399735	-0.432944	-2.779328
1	-2.458208	-0.867791	-0.128619	7	-1.347001	-0.883583	2.313715
1	0.754635	0.052629	-3.504585	7	2.841751	-0.500544	-0.177322
1	1.68668	-1.400164	-3.189867	7	-1.547799	-0.781608	-2.569596
1	2.304987	0.153675	-2.659394	8	3.474661	-1.155138	-0.992685
6	0.730091	-0.664364	0.998736	8	3.321537	0.203741	0.698298
6	-0.646569	-0.782893	1.016672	8	-0.658543	-0.86075	3.323182
6	-1.382696	-0.799534	-0.152696	8	-2.564711	-0.982781	2.284321
6	-0.701136	-0.724375	-1.355556	8	-2.607727	-0.174823	-2.533999
6	0.693755	-0.609698	-1.463028	8	-1.14092	-1.451907	-3.507164
6	1.364308	-0.592195	-0.229936				

Table 8. Oscillation frequencies and IR intensities:

Frequency cm^{-1}	Intensity (KM/Mol)	Frequency cm^{-1}	Intensity (KM/Mol)	Frequency cm^{-1}	Intensity (KM/Mol)	Frequency cm^{-1}	Intensity (KM/Mol)
43.8966	0.4182	468.0219	1.6456	955.9036	1.6191	1482.4453	7.5838
46.6024	0.0047	475.7409	0.1431	956.8704	12.4671	1502.2843	9.9084
51.1211	0.3465	538.8592	2.232	1050.7593	1.5785	1577.2756	222.6215
91.7581	5.6023	545.7044	2.7367	1056.2278	1.0227	1585.705	7.1251
116.369	4.314	656.0195	8.947	1097.7349	49.9934	1589.2693	403.4066
148.7023	2.786	668.7824	0.041	1183.8999	11.0977	1637.5889	101.4945
176.8952	0.7688	717.5582	19.2697	1216.2209	0.5961	1645.7786	95.2222
181.9206	0.0608	736.9124	51.5331	1222.8699	12.71	3073.4741	1.3805
182.8245	5.2877	755.0063	29.2922	1337.1632	1.8692	3133.1826	4.432
285.2091	3.1967	788.6055	0.2151	1367.5665	355.2155	3158.8633	4.1296
313.9959	0.301	792.709	3.0718	1377.3833	310.4697	3242.5811	15.8411
319.6074	0.2845	806.3562	13.7704	1386.6946	1.9108	3242.615	29.3568
353.2167	2.4823	839.2241	2.1683	1423.3486	7.5033		
357.4319	2.2329	916.6206	28.8523	1426.8933	9.487		
374.6578	0.1843	945.1449	33.0434	1476.3379	8.1678		

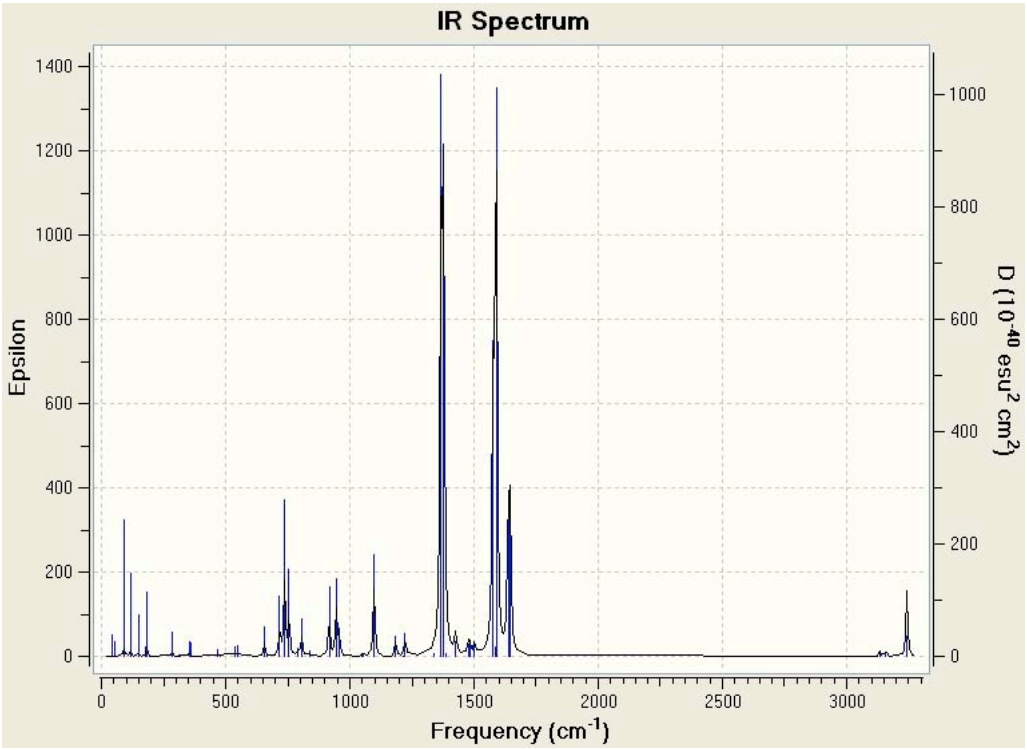

Figure 11. IR intensity as a function of frequency calculated using DFT B3LYP/6-311++G(2d,2p) for TNT1 according to frozen phonon approximation.

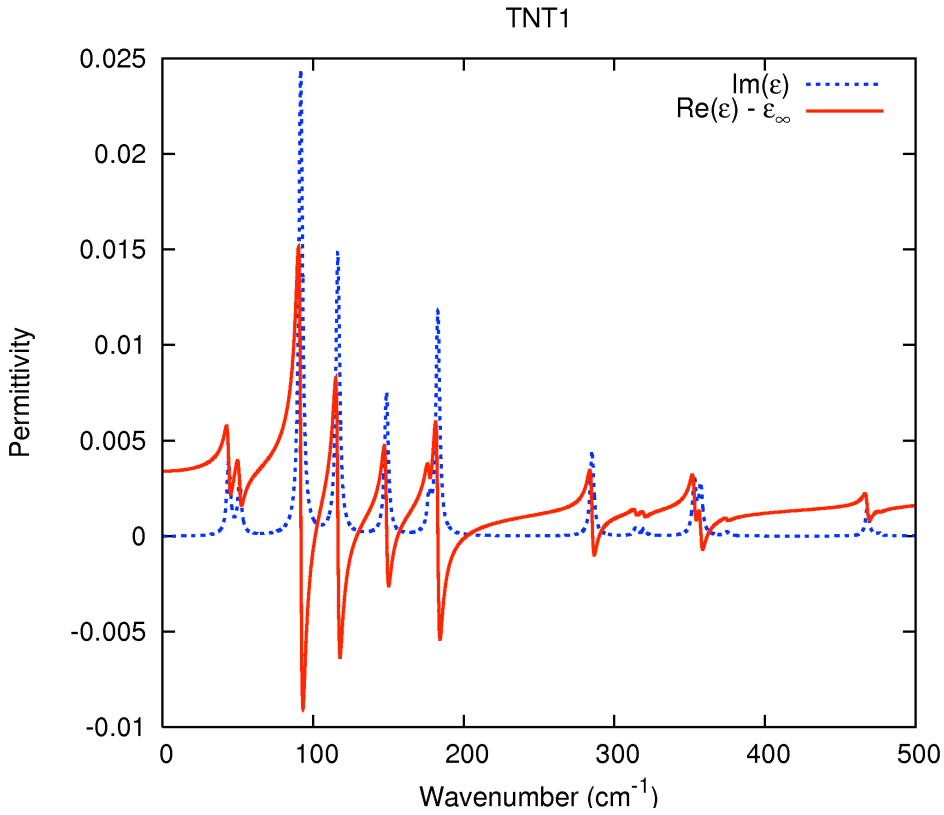

Figure 12. Real (solid) and imaginary (dashed) parts of permittivity function of TNT1 molecules with $\gamma_n = 3\ \mathrm{cm}^{-1}$ and $\rho = 2.4 \cdot 10^{19}\ \mathrm{cm}^{-3}$ for frequencies within THz range.

Case Study 5: TNT2

In this section are presented two sets of data, which are the results of computational experiments using DFT, concerning the molecule TNT2. These are the relaxed or equilibrium configuration of a single isolated molecule of TNT2 (see Table 9) and ground-state oscillation frequencies and IR intensities for this configuration that are calculated by DFT according to the frozen phonon approximation (see Table 10). The DFT model and basis function used for these calculations are the same as those used in case study 1. A schematic representation of the molecular geometry of TNT2 is shown in Fig.(13).

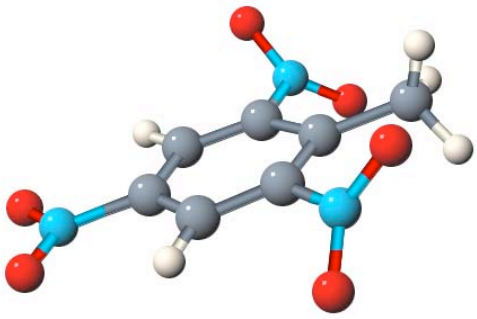

Figure 13. Molecular Geometry of TNT2.

Shown in Fig.(14) is the IR intensity as a function of frequency calculated using DFT for TNT2 according to a frozen phonon approximation. For the spectrum shown in Fig.(14), the structure of each resonance response is approximated essentially by that of a delta function.

Table 9. Atomic positions of TNT2 (Å):

Atomic number	X	Y	Z	Atomic number	X	Y	Z
1	1.272638	-0.725622	1.937201	6	1.414562	-0.48061	-2.757522
1	-2.47618	-0.756181	-0.127018	7	-1.38262	-0.826509	2.318558
1	0.783524	-0.783344	-3.582949	7	2.827982	-0.47615	-0.137647
1	2.308659	-1.100179	-2.762622	7	-1.555219	-0.729874	-2.559208
1	1.745243	0.546032	-2.910146	8	3.370156	0.303405	-0.907211
6	0.710963	-0.694766	1.017803	8	3.395655	-1.156863	0.702976
6	-0.669911	-0.747063	1.027129	8	-0.702058	-0.818858	3.333474
6	-1.398471	-0.726939	-0.147069	8	-2.602448	-0.894081	2.279716
6	-0.705392	-0.681604	-1.344792	8	-2.471574	0.074847	-2.615511
6	0.690578	-0.591628	-1.44343	8	-1.301622	-1.585811	-3.393552
6	1.352575	-0.590481	-0.204408				

Table 10. Oscillation frequencies and IR intensities:

Frequency cm^{-1}	Intensity (KM/Mol)	Frequency cm^{-1}	Intensity (KM/Mol)	Frequency cm^{-1}	Intensity (KM/Mol)	Frequency cm^{-1}	Intensity (KM/Mol)
42.0597	0.5991	411.8908	0.9361	952.4309	12.6243	1486.6581	6.208
46.8624	0.0008	504.5207	4.3108	955.8323	4.7116	1511.8199	17.3952
54.1237	0.175	542.3399	2.6744	1046.9528	2.0737	1577.0751	203.8374
73.6054	4.3526	580.5687	0.4432	1062.375	3.8168	1587.4009	280.5907
112.748	4.0026	597.2664	0.2412	1099.163	45.3744	1591.2745	207.5624
145.2265	1.5182	691.0656	23.9547	1184.0508	13.0568	1636.2683	98.2833
151.6023	2.6227	722.2813	4.3961	1216.8298	0.1771	1644.4102	52.6965
176.271	4.5499	737.6184	52.5565	1225.9679	11.4654	3071.1985	0.2464
179.9933	0.2715	763.4611	24.2778	1333.5236	1.7359	3120.1721	2.3101
278.5363	2.7931	774.787	5.025	1367.8151	356.8663	3186.2969	3.0995
308.1643	0.9928	798.3304	0.8215	1379.8845	270.1632	3238.0894	19.668
316.5652	0.4201	805.6322	13.5669	1392.578	42.5101	3243.6443	22.7845
349.3323	1.3951	839.0777	2.2141	1421.7412	11.0304		
354.8972	2.8862	915.717	30.5435	1428.6144	9.6139		
392.2231	2.6389	944.7272	29.7742	1474.3002	0.6607		

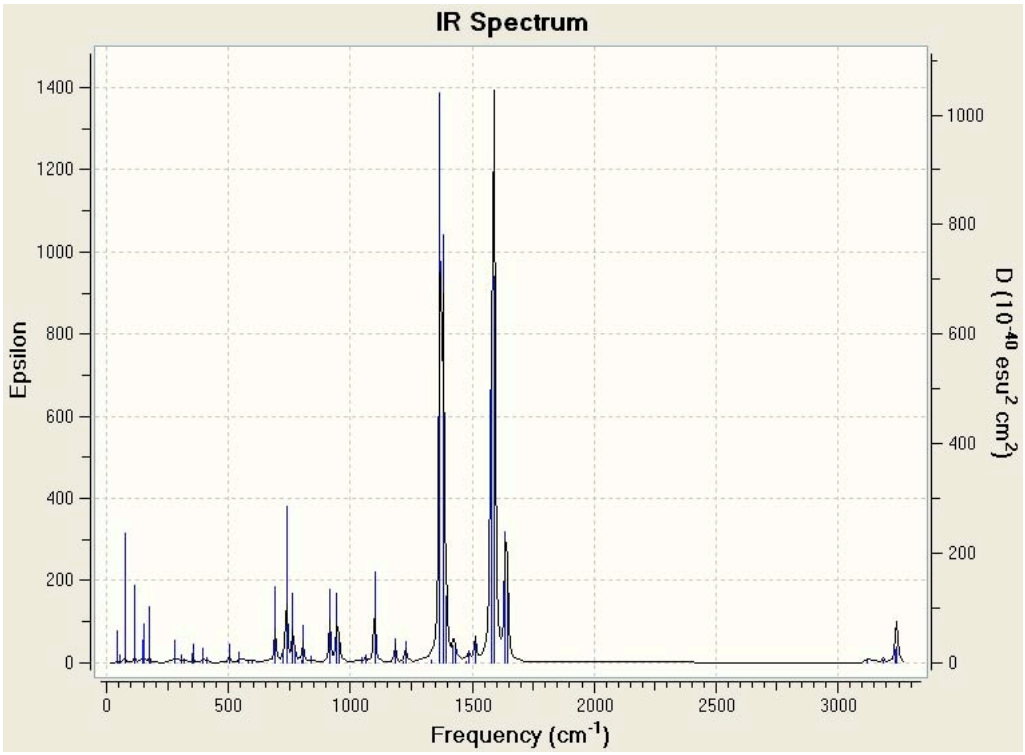

Figure 14. IR intensity as a function of frequency calculated using DFT B3LYP/6-311++G(2d,2p) for TNT2 according to frozen phonon approximation.

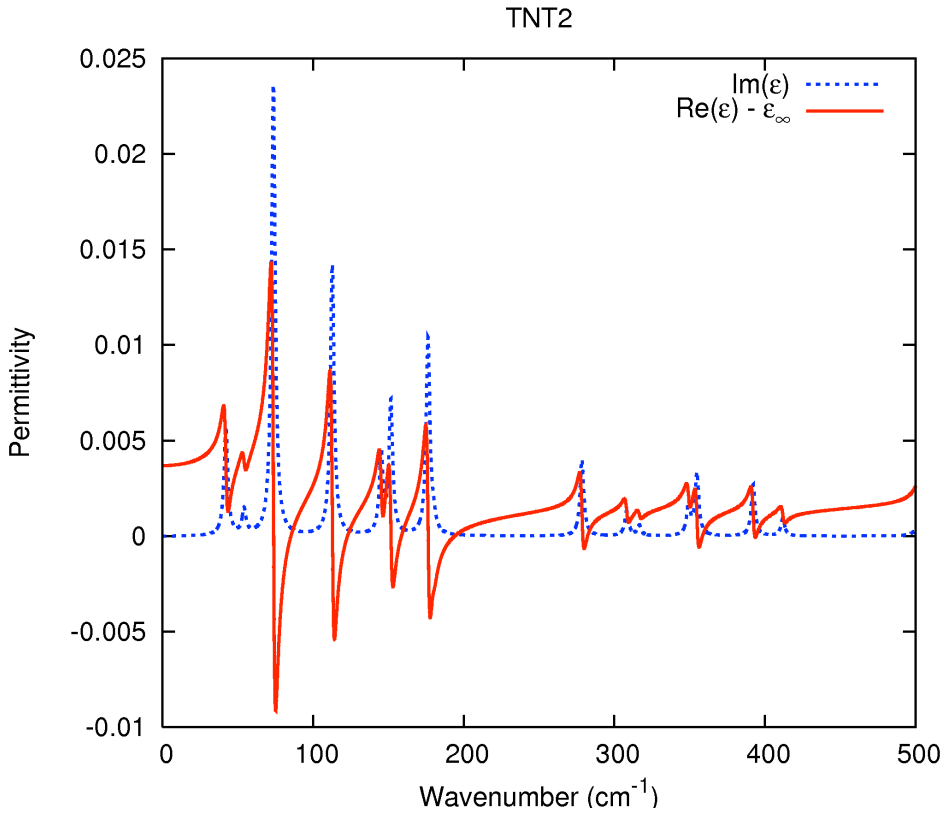

Figure 15. Real (solid) and imaginary (dashed) parts of permittivity function of TNT2 molecules with $\gamma_n = 3$ cm^{-1} and $\rho = 2.4 \cdot 10^{19}$ cm^{-3} for frequencies within THz range.

Discussion

The DFT calculated absorption spectra given in tables 2, 4, 6 and 8 provide two types of information for general analysis of dielectric response. These are the denumeration of ground state resonance modes and estimates of molecular level dielectric response structure. The construction of permittivity functions using the DFT calculated absorption spectra follows the same procedure as that applied for the construction of permittivity functions using experimentally measured absorption spectra, but with the addition of certain constraint conditions. Accordingly, construction of permittivity functions using either DFT or experimentally measured absorption spectra requires parameterizations that are in terms of physically consistent analytic function representations such as the Drude-Lorentz model. Although the formal structure of permittivity functions constructed using DFT and experimental measurements are the same, their interpretation with respect to parameterization is different for each case.

Conclusion

The calculations of ground state resonance structure associated with the high explosives β-HMX, PETN, RDX, TNT1 and TNT2 using DFT are meant to serve as reasonable estimates of molecular level response characteristics, providing interpretation of dielectric response features, for subsequent adjustment relative to experimental measurements and molecular structure theory.

Acknowledgement

This work was supported by the Office of Naval Research.

References

[1] M. J. Frisch, G. W. Trucks, H. B. Schlegel, G. E. Scuseria, M. A. Robb, J. R. Cheeseman, G. Scalmani, V. Barone, B. Mennucci, G. A. Petersson, H. Nakatsuji, M. Caricato, X. Li, H. P. Hratchian, A. F. Izmaylov, J. Bloino, G. Zheng, J. L. Sonnenberg, M. Hada, M. Ehara, K. Toyota, R. Fukuda, J. Hasegawa, M. Ishida, T. Nakajima, Y. Honda, O. Kitao, H. Nakai, T. Vreven, J. A. Montgomery, Jr., J. E. Peralta, F. Ogliaro, M. Bearpark, J. J. Heyd, E. Brothers, K. N. Kudin, V. N. Staroverov, R. Kobayashi, J. Normand, K. Raghavachari, A. Rendell, J. C. Burant, S. S. Iyengar, J. Tomasi, M. Cossi, N. Rega, J. M. Millam, M. Klene, J. E. Knox, J. B. Cross, V. Bakken, C. Adamo, J. Jaramillo, R. Gomperts, R. E. Stratmann, O. Yazyev, A. J. Austin, R. Cammi, C. Pomelli, J. W. Ochterski, R. L. Martin, K. Morokuma, V. G. Zakrzewski, G. A. Voth, P. Salvador, J. J. Dannenberg, S. Dapprich, A. D. Daniels, Ö. Farkas, J. B. Foresman, J. V. Ortiz, J. Cioslowski, and D. J. Fox, Gaussian 09, Revision A.1, Gaussian, Inc., Wallingford CT, 2009.

[2] A. Frisch, M. J. Frisch, F. R. Clemente and G. W. Trucks, Gaussian 09 User's Reference, pp105-106 (2009)

[3] P. Hohenberg and W. Kohn, "Inhomogeneous Electron Gas" Phys. Rev. **136**, B864, (1964).

[4] W. Kohn and L. J. Sham, "Self-Consistent Equations Including Exchange and Correlation Effects" Phys. Rev. **140**, A1133 (1965).

[5] R.O. Jones and O. Gunnarsson, "The density functional formalism, its applications and prospects" Rev. Mod. Phys. **61**, 689 (1989).

[6] W.W. Hager and H. Zhang, "A survey of nonlinear conjugate gradient methods," Pacific J. Optim., 2, p. 35-58 (2006).

[7] R. M. Martin, *Electronic Structures Basic Theory and Practical Methods*, Cambridge University Press, Cambridge 2004, p. 25.

[8] E. B. Wilson, J. C. Decius and P. C. Cross, *Molecular Vibrations* (McGraw-Hill, New York, 1955).

[9] J.W. Ochterski, "Vibrational Analysis in Gaussian," help@gaussian.com, 1999.

[10] C. A. D. Roeser and E. Mazur, "Light-Matter Interactions on Femtosecond Time Scale" in *Frontiers of Optical Spectroscopy*, eds. B. Di Bartolo and O. Forte, NATO Science Series v. 168 p. 29, Kluwer Academic Publishers, Dordrecht – Norwell, 2005; C. F. Bohren and D. R. Huffman, *Absorption and Scattering of Light by Small Particles* (Wiley-VCH Verlag, Weinheim, 2004).

[11] A. D. Becke, "Density-funtional Thermochemistry. III. The Role of Exact Exchange", *J. Chem. Phys.* **98**, 5648-5652 (1993).

[12] B. Miehlich, A. Savin, H. Stoll and H. Preuss, "Results of Obtained with the Correlation Energy Density Functionals of Becke and Lee, Yang and Parr", Chem. *Phys. Lett.* **157**, 200-206 (1989).

[13] A. D. McLean and G. S. Chandler, "Contracted Gaussian-basis sets for molecular calculations. 1. 2nd row atoms, Z=11-18," *J. Chem. Phys.*, **72** 5639-48 (1980)

[14] T. Clark, J. Chandrasekhar, G. W. Spitznagel and P. v. R. Schleyer, "Efficient diffuse function-augmented basis-sets for anion calculations. 3. The 3-21+G basis set for 1st-row elements, Li-F," *J. Comp. Chem.*, **4** 294-301, (1983).

[15] M. J. Frisch, J. A. Pople and J. S. Binkley, "Self-Consistent Molecular Orbital Methods. 25. Supplementary Functions for Gaussian Basis Sets," *J. Chem. Phys.*, **80** (1984) 3265-69.